Full-duplex Spectrum Sensing and Fairness Mechanisms for Wi-Fi/LTE-U Coexistence

Mohammed Hirzallah, Wessam Afifi, and Marwan Krunz
Department of Electrical and Computer Engineering, University of Arizona, AZ, USA
{hirzallah, wessamafifi, krunz}@email.arizona.edu

***Abstract*—In this paper, we investigate the coexistence problem between Wi-Fi and a pre-standard form of LTE over unlicensed bands, namely, LTE-Unlicensed (LTE-U). We address two coexistence problems. First, the different access mechanisms for Wi-Fi and LTE-U can lead to an increase in the collision rate and higher latency for both systems. We propose a modified Wi-Fi operation mode, whereby Wi-Fi stations (STAs) carry out simultaneous spectrum sensing and transmission to reduce the time required for collision detection. Specifically, we propose and analyze a full-duplex (FD) based detection framework that can differentiate between Wi-Fi and LTE-U signals while taking into account residual self-interference. Second, the ability to differentiate between Wi-Fi and LTE-U signals motivates the idea of adapting the clear channel assessment (CCA) threshold according to the type of the detected signal. Inspired by upcoming Wi-Fi standards (e.g., IEEE 802.11ax), we propose a CCA threshold adaptation scheme and study via simulations its optimal setting so as to maximize the spatial reuse while maintaining fairness between LTE-U and Wi-Fi systems.**

***Index Terms*—Wi-Fi/LTE-U coexistence, full-duplex, simultaneous transmission-sensing, CCA threshold adaptation.**

I. Introduction

The anticipated 1000x increase in wireless demand between 2010 and 2020, prompted the FCC to open up parts of the 5 GHz band for unlicensed access. Given the proximity of this band to their licensed spectrum, wireless operators became quite interested in extending the benefits of LTE-A to the unlicensed spectrum (LTE-U). The main idea behind LTE-U is to exploit the carrier aggregation (CA) feature in LTE-A systems to combine licensed LTE 4G spectrum and unlicensed 5 GHz spectrum, targeting higher downlink (DL) throughput for LTE users. Coexistence between heterogeneous systems (e.g., LTE-U and Wi-Fi) in the unlicensed 5 GHz band is particularly challenging due to the difference in the access mechanism used by both systems. In particular, Wi-Fi systems are contention based whereas LTE/LTE-U systems are schedule based. Such heterogeneity may lead to higher collision rate and latency.

In an effort to reduce the LTE-U impacts over Wi-Fi system, two LTE approaches have been proposed: The schedule-based LTE-U [1] and the contention-based LTE-U [2](e.g., licensed assisted access (LAA)). LTE-U accesses spectrum in a time division multiplexing based fashion (see Figure 1). LTE-U measures active Wi-Fi transmission during the OFF period and adjusts its duty cycle accordingly. Because LTE-U is expected to be a starting short-term approach in some countries such as US and China, in this paper, we focus on the coexistence problem between Wi-Fi and LTE-U systems.

This research was supported in part by the National Science Foundation (grants number IIP-1535573, IIP-1265960, and CNS-1563655). Any opinions, findings, conclusions, or recommendations expressed in this paper are those of the author(s) and do not necessarily reflect the views of NSF.

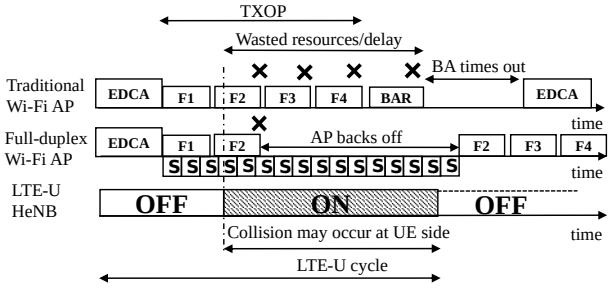

Fig. 1: Collision between LTE-U and TXOP Wi-Fi transmission (S stands for sensing, F stands for frame).

In IEEE 802.11 standards, stations (STAs) contend using the enhanced distributed channel access (EDCA) scheme, which is an extension to the well-known distributed coordination function (DCF). The successful STA can reserve the channel for a duration called a transmit opportunity (TXOP). During a TXOP, a Wi-Fi access point (AP) or STA may exchange multiple of frames (see Figure 1). At the end of the TXOP, the transmitting AP transmits a block ACK request (BAR) to the receiving STA, which replies with a block ACK (BA) signaling correct reception [3]. A TXOP may last up to 3.008ms.

LTE-U implementation may lead to severe service degradation for traditional Wi-Fi users, since the home eNodeB (HeNB) may start its transmission and collide AP transmission. As shown in Figure 1, traditional AP detects the failure of its transmission after the BA times out resulting in long delays, reduced throughput, and power loss for both systems (e.g., frames F2 – F4 are lost, but AP only knows about it after TXOP ends). In this paper, we propose to equip Wi-Fi STAs with self-interference suppression (SIS) capabilities to enable *simultaneous transmission and sensing* (STS). This so-called full-duplex (FD) sensing provides Wi-Fi device with more awareness about neighboring systems. If an LTE-U signal is sensed, Wi-Fi device can back off earlier avoiding long delay due to collision or switch to another idle channel.

FD sensing was previously explored for oppotunisitic dynamic spectrum access (DSA) systems using energy- [4, 5] and waveform- [6] based detection. Energy detection cannot differentiate between types of different signals (e.g., LTE-U vs. Wi-Fi). Given that Wi-Fi and LTE-U signals are both OFDM modulated, our goal is to harness their unique features to distinguish between them. The authors in [7–9] exploited the cyclic prefix (CP) of OFDM symbols for signal detection, but only for half-duplex (HD) systems (i.e., sensing only where no residual interference exists). Authors in [10] proposed

equipping LTE devices with FD capabilities to sense Wi-Fi signals using cyclostationarity, but did not discuss leveraging their scheme for improving the performance of other coexistent systems. The previous literature, except [7], require long detection time. In this paper, we propose and analyze an FD sensing approach for coexisting Wi-Fi/LTE-U systems based on a two-sliding-window correlator scheme, which has relatively faster detection time.

In Wi-Fi systems, a STA compares the measured received signal strength with a clear channel assessment (CCA) threshold prior to its transmission. Channel is deemed to be busy when measured signal power exceeds CCA threshold. Upcoming Wi-Fi standards (e.g., 802.11ax) aim to enhance the spatial reuse by adapting CCA threshold value [11]. However, the specification framework document (SFD) does not discuss how Wi-Fi STAs should react when an LTE-U signal is detected. Differentiating between LTE-U and Wi-Fi signals motivates us to study the optimal CCA threshold setting that enhances the spatial reuse while maintaining fairness between Wi-Fi and LTE-U systems. For example, decreasing the CCA threshold for Wi-Fi STAs will make Wi-Fi more conservative and bias the network throughput towards LTE-U. On the other hand, increasing this threshold will make Wi-Fi STAs more aggressive in accessing the spectrum, which could be unfair to the LTE-U system. Our goal is to balance the aforementioned tradeoff by determining the optimal CCA threshold value.

Previous works on LTE-U/Wi-Fi coexistence addressed different issues, ranging from evaluating the performance of coexisting systems through experimentation [12], to analyzing it using stochastic geometry [13]. To the best of our knowledge, this is the first paper to incorporate FD techniques to enhance Wi-Fi TXOP mode performance within a Wi-Fi/LTE-U coexistence framework and to discuss the optimal Wi-Fi CCA threshold setting with respect to LTE-U signals.

The contributions of this paper are as follows. First, we propose a modified TXOP scheme for Wi-Fi STAs with SIS capabilities, which enhances spectrum awareness and reduces the time required for collision detection. We derive the probabilities of detection and false-alarm under imperfect SIS, and propose a Neyman-Pearson (NP) detection rule. The proposed FD detector, on average, attains 10^{-3} mis-detection probability at -6 dB LTE-U signal-to-noise ratio. Second, to enhance the spatial reuse, we propose an adaptive CCA threshold scheme for Wi-Fi systems. We study via simulations the optimal CCA threshold value for Wi-Fi STAs, which improves the fairness of channel access for Wi-Fi and LTE-U small cells. Our study reveals that the optimal CCA threshold is a function of two factors: LTE-U duty cycle and LTE-U/Wi-Fi node densities.

II. System Model

We consider an LTE-U small cell that coexists with a Wi-Fi network in the 5 GHz unlicensed bands. The LTE-U small cell consists of an HeNB that communicates with a number of UEs over an aggregation of licensed and unlicensed channels. HeNB must search for a free channel to use. If no idle channel is found, HeNB shares the spectrum with the Wi-Fi system according to an adaptive duty cycling (see LTE-U HeNB activity in Figure 1). Without loss of generality, we focus on the LTE-U downlink. The Wi-Fi system consists of one FD-enabled AP that communicates with a number of STAs. Wi-Fi STAs (AP and non-AP) perform traditional CSMA/CA before accessing any of the available unlicensed channels.

The proposed TXOP operation mode is shown in Figure 1 (see Full-duplex Wi-Fi AP activity). The Wi-Fi AP performs simultaneous transmission and sensing for several consecutive frames. In this example, the AP detects an LTE-U signal while transmitting frame F2. Based on the the signal level of the detected LTE-U signal (discussed in Section IV), the AP may decide to back off until the next OFF period or switch to a new idle channel. We assume that the LTE-U, Wi-Fi, and noise signals at sampling time n, denoted by $l(n)$, $s(n)$, and $w(n)$, respectively, follow a symmetric circular complex Gaussian distribution: $l \sim \mathcal{N}_c(0, \sigma_l^2)$, $s \sim \mathcal{N}_c(0, \sigma_s^2)$, and $w \sim \mathcal{N}_c(0, \sigma_w^2)$, respectively. The interference at the FD-enabled Wi-Fi device can be expressed as follows:

$$r(n) = \Big(h_{lw}(n) * l(n)\Big) + \Big(\chi_w h_{ww}(n) * s(n)\Big) + w(n) \quad (1)$$

where $*$ is the convolution operation, h_{lw} is the channel gain between HeNB and the Wi-Fi AP (STA), and h_{ww} is the gain of the self-interference channel of Wi-Fi AP (the attenuation between the transmit and receive chain of the FD AP), and χ_w is the SIS capability of the Wi-Fi AP (perfect SIS occurs at $\chi_w = 0$). We assume a linear channel model, and hence channel outputs will remain normally distributed.

We focus on the detecting LTE-U signals at a Wi-Fi nodes. We introduce three metrics: the LTE-U interference-to-noise ratio (INR) σ_l^2/σ_w^2, which quantifies the ratio of LTE-U signal level with respect to the power of Wi-Fi noise floor, the inter-symbol-interference (ISI) ISI-to-noise ratio (ISNR) $\beta^2\sigma_{\tilde{l}}^2/\sigma_w^2$ ($\sigma_{\tilde{l}}^2$ is the power of previous received LTE-U symbol, β models ISI). ISNR quantifies how much ISI that LTE-U signal suffers with respect to the power of Wi-Fi noise floor, and the self-interference-to-noise ratio (STNR) $\chi_w^2\sigma_s^2/\sigma_w^2$, which quantifies the Wi-Fi residual self interference (RSI) power level with respect to that of Wi-Fi noise floor.

III. Cyclic-Prefix-Based Detection

LTE-U and Wi-Fi signals are OFDM modulated, where each OFDM symbol consists of a data part and a pre-appended CP (see Figure 2). CP is a replication of some data symbols, and it is added to mitigate the ISI and facilitate synchronization at receivers. CP is most likely to be contaminated by ISI. Consider an LTE-U signal with OFDM symbol structure consisting of N data and L CP samples. At the Wi-Fi receiver, the received analog signal is passed through the analog-to-digital (ADC) converter to obtain discrete samples. Later on, these samples are partitioned into two windows, W_1 and W_2, of length L and a timing difference equals $N - L$. We slide these two windows structure over all received samples (see Figure 2). We call the time instant for which window W_1 aligns with LTE-U's samples corresponding to CP the *optimal time*, and other times as *regular times*. We correlate samples in these windows using a timing metric that will be presented shortly, and compare correlation value with a predefined threshold. At the optimal time, the correlation exceeds the threshold and a presence of an LTE-U signal is indicated, while at regular times the correlation value will be lower than the threshold. We propose the following correlation timing metric:

$$M_\tau(n) = \frac{|A(n)|^2}{(\max(E_1(n), E_2(n)))^2} \quad (2)$$

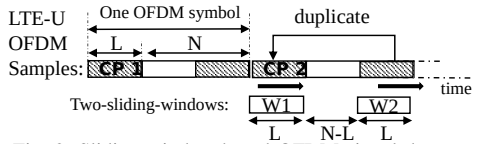

Fig. 2: Sliding-window-based OFDM signal detector.

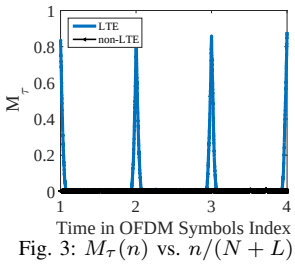

Fig. 3: $M_\tau(n)$ vs. $n/(N+L)$.

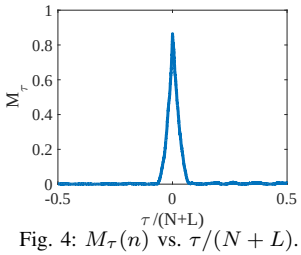

Fig. 4: $M_\tau(n)$ vs. $\tau/(N+L)$.

where $A(n)$ is the correlation between samples in the two windows, and $E_1(n)$ and $E_2(n)$ are the energies of the samples in the two windows, respectively:

$$\begin{aligned} A(n) &= \textstyle\sum_{k=0}^{L-1} r(n-k)r^*(n-k-N) \\ E_1(n) &= \textstyle\sum_{k=0}^{L-1} r(n-k-N)r^*(n-k-N) \\ E_2(n) &= \textstyle\sum_{k=0}^{L-1} r(n-k)r^*(n-k) \end{aligned} \tag{3}$$

where r^* indicates the complex conjugate of r. The τ index in M_τ indicates the alignment of the sliding windows with respect to the starting point of the OFDM symbol (i.e, CP). τ takes integer values in the period $(-(N+L)/2, (N+L)/2]$, with $\tau = 0$ corresponding to the optimal time, while $\tau > L$ corresponds to regular times.

Figure 3 shows $M_\tau(n)$ as a function of the OFDM symbol index, when four symbols are detected. Figure 4 depicts $M_\tau(n)$ as a function of misalignment index τ. Both figures are generated with INR = 25 dB, $L = 500$, $N = 6400$, and ISNR = 6 dB. The hypothesis testing can be defined as follows:

$$r(n)=\begin{cases} \chi_w s(n) + w(n), \text{ under } \mathcal{H}_0 \\ l(n)+\chi_w s(n)+w(n), \text{ under } \mathcal{H}_0,\ n \text{ is a regular time} \\ l(n)+\chi_w s(n)+w(n), \text{ under } \mathcal{H}_1, n \text{ is the optimal time} \end{cases}$$

where the first two lines represent the null hypothesis $\mathcal{H}_0$, and the third line represents the alternate hypothesis $\mathcal{H}_1$. Define the general detection rule as:

$$\tilde{\delta}(r(n)) = \begin{cases} 1 & \text{, if } M_\tau(n) \geq \lambda_{th} \\ 0 & \text{, if } M_\tau(n) < \lambda_{th}. \end{cases} \tag{4}$$

Before proposing the NP rule that selects the threshold λ_{th}, we first derive $M_\tau(n)$ statistics under different hypotheses.

A. Statistics at the Optimal Time

According to (1), at $\tau = 0$, the received samples in the two-sliding-window at Wi-Fi AP receiver are:

$$\begin{aligned} r(k-N) &= \beta\tilde{l}(k-N) + l(k-N) + \chi_w s(k-N) + w(k-N) \\ r(k) &= l(k) + \chi_w s(k) + w(k) \end{aligned} \tag{5}$$

where $k \in \{n-L+1, \cdots, n\}$, $r(k-N)$ and $r(k)$ represent the samples in the first and second windows, respectively, and $\tilde{l}$ denotes samples from the previously transmitted OFDM symbol that overlap with the current received OFDM symbol due to ISI. We drop the channel dependence in (1), since the channel will not change the distribution of the transmitted samples. $l(k-N)$ in (5) belongs to the CP, while $l(k)$ belongs to CP's original duplicated part, and both have equal magnitude. $l(k-N)$ and $\tilde{l}(k-N)$ are independent, since they belong to two different LTE OFDM symbols. We assume the noise samples to be independent and identically distributed, so $w(k-N)$ and $w(k)$ are also independent. For colored noise, pre-whiting techniques can be applied. $A(n)$ in (3) can be written as $A(n) = \sum_{k=n-L+1}^{n} A_k$, and accordingly the mean $\mu_{Ak} = E[A_k] = \sigma_l^2$ and the variance σ_{Ak}^2 is evaluated as:

$$\begin{aligned} \sigma_{Ak}^2 = 3\sigma_l^4 + \sigma_w^4 + \chi_w^4\sigma_s^4 + \beta^2\sigma_{\tilde{l}}^2\sigma_l^2 + \beta^2\sigma_{\tilde{l}}^2\sigma_w^2 + \chi_w^2\beta^2\sigma_{\tilde{l}}^2\sigma_s^2 \\ + 2\sigma_l^2\sigma_w^2 + 2\chi_w^2\sigma_s^2\sigma_l^2 + 2\chi_w^2\sigma_s^2\sigma_w^2 - \mu_{Ak}^2. \end{aligned} \tag{6}$$

By the central limit theorem (CLT), for large L, $A(n)$ will be normally distributed with mean of $\mu_A = L\mu_{Ak}$ and variance $\sigma_A^2 = L\sigma_{Ak}^2$. In practice, at the optimal time, $A(n)$ will be composed of a dominant real part and a small imaginary part.

The statistics and distribution for the denominator in (2) can be derived by finding the mean and variance of E_1 and E_2. It is straightforward to show that E_1 and E_2 are normally distributed $E_1 \sim \mathcal{N}(L\mu_{E1,k}, L\sigma_{E1,k}^2)$, $E_2 \sim \mathcal{N}(L\mu_{E2,k}, L\sigma_{E2,k}^2)$, where the mean $\mu_{E2,k} = \sigma_l^2 + \chi_w^2\sigma_s^2 + \sigma_w^2$, variance $\sigma_{E2,k}^2 = 2\mu_{E2,k}^2$, $\mu_{E1,k} = \beta^2\sigma_{\tilde{l}}^2 + \mu_{E2,k}$, and $\sigma_{E1,k}^2 = 2\mu_{E1,k}^2$. For low ISI conditions (e.g., ISNR $\leq$ INR), E_1 and E_2 have almost similar statistics, and accordingly $Z(n) \triangleq \max(E_1(n), E_2(n))$ is normally distributed, $Z \sim \mathcal{N}(\mu_z, \sigma_z^2)$, where the mean μ_z and the variance $\sigma_z^2 = \mathrm{E}[Z^2] - \mu_z^2$ are derived as in [14]:

$$\begin{aligned} \mu_z &= \mu_{E1}\Phi(\eta) + \mu_{E2}\Phi(-\eta) + \theta_{12}\phi(\eta) \\ \mathrm{E}[Z^2] &= (\sigma_{E1}^2 + \mu_{E1}^2)\Phi(\eta) + (\sigma_{E2}^2 + \mu_{E2}^2)\Phi(-\eta) \\ &\quad + (\mu_{E1} + \mu_{E2})\theta_{12}\phi(\eta) \end{aligned} \tag{7}$$

where $\Phi(\cdot)$ and $\phi(\cdot)$ are the CDF and PDF of the standard normal function, $\eta = (\mu_{E1} - \mu_{E2})/\theta_{12} = \beta^2\sigma_{\tilde{l}}^2 L/\theta_{12}$, and $\theta_{12} = \sqrt{\sigma_{E1}^2 + \sigma_{E2}^2 - 2\rho_{12}\sigma_{E1}\sigma_{E2}}$. The correlation coefficient ρ_{12} represents the correlation index between E_1 and E_2, $\rho_{12} = (\mathrm{E}[E_1E_2] - \mu_{E1}\mu_{E2})/(\sigma_{E1}\sigma_{E2})$. Let $b = \sigma_w^4 + \chi_w^4\sigma_w^4 + \beta^2\sigma_{\tilde{l}}^2\sigma_l^2 + \beta^2\sigma_{\tilde{l}}^2\sigma_w^2 + \chi_w^2\beta^2\sigma_{\tilde{l}}^2\sigma_s^2 + 2\sigma_l^2\sigma_w^2 + 2\chi_w^2\sigma_l^2\sigma_s^2 + 2\chi_w^2\sigma_w^2\sigma_s^2$, then $\mathrm{E}[E_1E_2] = L(3\sigma_l^4 + b) + (L^2 - L)(\sigma_l^4 + b)$.

Let $Q(n) \triangleq A(n)/Z(n)$. Then, $Q(n)$ is the ratio of two normal random variables. For small standard deviation to mean ratios for $A(n)$ and $Z(n)$, $Q(n)$ has approximately a normal distribution, $Q(n) \sim \mathcal{N}(\mu_Q, \sigma_Q^2)$ [15], where the mean μ_Q, and the variance σ_Q^2 can be approximated with the help of Taylor series as in [16]:

$$\begin{aligned} \mu_Q &= \mathrm{E}[\frac{A}{Z}] \approx \frac{\mu_A}{\mu_Z} + \mathrm{Var}(Z)\frac{\mu_A}{\mu_Z^3} - \frac{\mathrm{Cov}(AZ)}{\mu_Z^2} \\ \sigma_Q^2 &\approx \Big(\frac{\mathrm{Var}(A)}{\mu_Z^2} + \frac{\mu_A^2\mathrm{Var}(Z)}{\mu_Z^4} - \frac{2\mu_A\mathrm{Cov}(AZ)}{\mu_Z^3}\Big) \end{aligned}$$

where $\mathrm{Cov}(AZ) = \mathrm{E}[AZ] - \mu_A\mu_Z$ is the covariance between A and Z, and $\mathrm{E}[AZ]$ can be evaluated as follows:

$$\mathrm{E}[AZ] = \mathrm{E}[AE_1]\Pr[E_1 > E_2] + \mathrm{E}[AE_2]\Pr[E_2 > E_1].$$

We found through simulations that, on average, $\Pr[E_1 > E_2] \approx 1$ when LTE-U signal level with respect to ISI satisfies INR $-$ STNR $\leq$ 15 dB. Let $c = \sigma_l^4 + \sigma_l^2\sigma_w^2 + \chi_w^2\sigma_w^2\sigma_s^2$, then $\mathrm{E}[AE_1] = 3L(c + \beta^2\sigma_{\tilde{l}}^2\sigma_l^2) + (L^2 - L)(c + \beta^2\sigma_{\tilde{l}}^2\sigma_l^2)$ and $\mathrm{E}[AE_2] = 3Lc + c(L^2 - L)$.

The last step is to evaluate the distribution of $M_{\tau=0}(n) \triangleq |Q(n)|^2$, which is the square of a normal random variable.

$M_{\tau=0}$ has a chi-square distribution; however, for small $Q(n)$'s variance-to-mean ratio, $M_{\tau=0}$ can be approximated as a normal random variable [17]:

$$M_{\tau=0} \sim \Big(\mu_Q + N(0,\sigma_Q^2)\Big)^2 \approx \mu_Q^2 + 2\mu_q N(0,\sigma_Q^2)$$

with mean $\mu_{M_{\tau=0}} = \mu_Q^2$, and variance $\sigma^2_{M_{\tau=0}} = 4\mu_Q^2\sigma_Q^2$.

The probability of detection for a threshold λ_{th} is:

$$\mathrm{Pd}\,(\lambda_{th}) = \Pr\left[\{M_{\tau=0} \geq \lambda_{th} | \mathcal{H}_1\}\right] = \mathcal{Q}\Big(\frac{\lambda_{th} - \mu_{M_{\tau=0}}}{\sigma_{M_{\tau=0}}}\Big) \quad (8)$$

where $\mathcal{Q}(\cdot)$ is the complementary cumulative function of the standard normal distribution.

B. Statistics at Regular Times

At regular times, the samples in the two-sliding-window are formulated as in (5) by dropping the $\beta\tilde{l}(k-N)$ term. $r(k)$ and $r(k-N)$ are independent samples. The correlation process in (3) results in summing complex random samples, and for large L, by CLT, $A(n)$ will be composed of real and imaginary parts that are independent and normally distributed. The mean and variance of $A(n)$'s real and imaginary parts can be derived in a similar way we did in (6), and they will have a zero mean and a variance of $L(\sigma_l^2 + \sigma_w^2 + \chi_w^2\sigma_s^2)^2/2 = L\mu_{E2,k}^2/2$. $|A(n)|^2$ is the sum of the squares of two normal random variables, and hence $|A(n)|^2$ will be chi-square distributed, and with an appropriate scaling it will be:

$$|A(n)|^2 \sim L(\mu_{E2,k})^2 \mathcal{X}_2^2 \quad (9)$$

where $\mathcal{X}_2^2$ is the chi-square distribution.

$Z(n)$ has a normal distribution $Z \sim \mathcal{N}(\mu_Z, \sigma_Z^2)$. The mean and variance of $E_1(n)$, $E_2(n)$, and $Z(n)$ can be derived in a similar way as we did before at the optimal time in (7), except the fact that the correlation coefficient ρ_{12} is zero. These entities remain normally distributed, and their statistics are $\mu_{E1} = \mu_{E2} = L\mu_{E2,k}$, $\sigma_{E1}^2 = \sigma_{E2}^2 = 2L\mu_{E2}^2$, $\mu_z = (L + 0.7978\sqrt{L})\mu_{E2}$, and $\sigma_Z^2 = (L^2 + 3.128L)\mu_{E2}^2$.

$Z^2(n)$ is the square of a normal random variable and has chi-square distribution. $Z^2(n)$ can be approximated with a normal distribution [17]:

$$\begin{aligned} Z^2 &\sim (\mu_Z + \mathcal{N}(0,\sigma_Z^2))^2 = \mu_Z^2 + 2\mu_Z\mathcal{N}(0,\sigma_Z^2) \\ &+ (\mathcal{N}(0,\sigma_Z^2))^2 \approx \mathcal{N}(\mu_Z^2, 4\mu_Z^2\sigma_Z^2). \end{aligned} \quad (10)$$

The timing metric at the regular time $M_{\tau>L}$ is the ratio of the distributions in (9) and (10):

$$\begin{aligned} M_{\tau>L} &\sim L\mu_{E2}^2 \frac{\mathcal{X}_2^2}{\mathcal{N}(\mu_Z^2, 4\mu_Z^2\sigma_Z^2)} \\ &\approx \frac{L\mu_{E2}^2}{\mu_Z^2}\Big[\mathcal{X}_2^2 - \mathcal{N}(0, 4\frac{\sigma_Z^2}{\mu_Z^2})\Big] \approx a_1\mathcal{X}_2^2 \end{aligned} \quad (11)$$

where $a_1 = L/(L + 0.7978\sqrt{L})^2$. We handle the previous approximations in a similar way to the analysis in [17]. The scaling in (11) results in a gamma distribution $\Gamma(\frac{k}{2}, 2a_1)$ with a shape parameter of $k/2 = 1$ and a scaling parameter of $2a_1$. As seen in (11) $M_{\tau>L}$ has a gamma distribution that is independent of the noise or signal statistical properties, $M_{\tau>L}$ distribution is only dependent on L, which depends on the length of CP for LTE-U signals and the sampling frequency of Wi-Fi AP.

False alarm probability for a detection threshold λ_{th} can be can be formulated according to the CDF of gamma distribution $F_{\gamma,1,2a_1}(\cdot)$ that has a shape parameter equals one and scale parameter equals to $2a_1$:

$$P_F(\lambda_{th}) = \Pr[\{M_{(\tau>L)} > \lambda_{th}\}|\mathcal{H}_0] = 1 - F_{\gamma,1,2a_1}(\lambda_{th}). \quad (12)$$

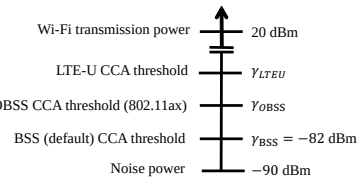

Fig. 5: Illustration of the proposed CCA adaptation scheme for W-fi systems.

C. Statistics in the Absence of OFDM Signal

In the absence of OFDM signal, we denote the timing metric by M_u. The samples in the two-sliding-window are formulated as in (5) by dropping $\beta\tilde{l}(k-N)$, $l(k)$, and $l(k-N)$ terms. M_u's distribution and statistics can be derived in a similar manner as we did for the regular time:

$$M_u \sim \frac{L(\sigma_w^2 + \chi_w^2\sigma_s^2)^2}{\mu_Z^2}\mathcal{X}_2^2 = \frac{L}{(L + 0.7978\sqrt{L})^2}\mathcal{X}_2^2 \quad (13)$$

where $\mu_z = \mu_{E1} + 0.3989\sqrt{2}\sigma_{E1}$, $\mu_{E1} = L(\sigma_w^2 + \chi_w^2\sigma_s^2)$, and $\sigma_{E1}^2 = 2L(\sigma_w^2 + \chi_w^2\sigma_s^2)^2$. M_u has a gamma distribution similar to the one derived before in (11), and hence it has a similar probability of false alarm as in (12).

D. NP Detection

We propose an NP detection rule based on the previous derived statistics. There are two sources of false alarms, the first happens when there is no LTE-U signal, while the second occurs at the *regular time*. Given the distributions in (11) and (13), then the NP detection threshold $\lambda_{th} = \lambda_{NP}$ in (4) is:

$$\lambda_{th} = \lambda_{NP} = F^{-1}_{\gamma,1,2a_1}(1-\alpha). \quad (14)$$

where α is the maximum false-alarm probability. The NP detector does not require any prior knowledge about neither signal nor noise statistical characteristics; it only requires the knowledge about the CP length (i.e., L).

IV. CCA Adaptation for Fair Coexistence

We propose a CCA adaptation scheme for Wi-Fi systems inspired by current proposals in 802.11ax SFD [11]. A key enabling technique for the proposed scheme is the sliding window correlator that can differentiate between LTE-U and Wi-Fi signals. Figure 5 shows an overview of the CCA adaptation map. Prior to IEEE 802.11ac (included), Wi-Fi STAs use the minimum CCA threshold (≈ -82 dBm) to determine whether a specific channel is idle or not. This conservative approach has been modified recently in 802.11ax SFD, which aims to increase the area throughput (i.e., enhance the spatial reuse) by increasing the CCA threshold for inter-BSS (i.e., OBSS) signals. BSS is the basic service set which is the basic network structure in Wi-Fi networks. Hence, $\gamma_{\text{OBSS}} > \gamma_{\text{BSS}} \approx -82$ dBm. The exact value for γ_{OBSS} is left as an implementation issue.

Since no discussion about LTE-U and Wi-Fi coexistence took place in 802.11ax SFD, we propose that Wi-Fi STAs exploit the proposed detection framework to adapt their CCA threshold value according to the detected signal type (BSS,

OBSS, or LTE-U). Algorithm 1 outlines the proposed adaptation structure for traditional HD sensing. We discuss the modifications needed for FD sensing at the end of the section.

As shown in Algorithm 1, before transmission, a Wi-Fi STA executes CCA by measuring the received signal strength indicator (RSSI) and compare it with $\gamma_{\text{BSS}} \approx -82$ dBm (i.e., energy detection). If no signal is detected, the Wi-Fi STA starts transmitting. On the other hand, if RSSI $> \gamma_{\text{BSS}}$, it needs to determine whether the detected signal is a Wi-Fi or an LTE-U signal, which can be done using the sliding window correlator. If the detected signal is LTE-U (e.g., $M > \lambda_{th}$), the Wi-Fi STA needs to measure the signal strength by comparing the RSSI with γ_{LTEU}. We assume that $\gamma_{\text{LTEU}} \geq \gamma_{\text{OBSS}}$ since a Wi-Fi STA can deal with an LTE-U signal (in terms of collocated transmission) at least as it deals with an OBSS signal. On the other hand, if the detected signal does not belong to a neighboring LTE-U small cell, the Wi-Fi STA has to determine whether the detected signal belongs to a BSS or an OBSS by checking the BSS color bits in the packet header. According to the signal type, the Wi-Fi STA can use either γ_{BSS} or γ_{OBSS}.

The sequence of the detection techniques in Algorithm 1 is important to minimize the sensing duration. Energy detection is used first to take a quick decision about channel availability since it does not require signal decoding. If a signal is detected, the sliding correlator has to be used before the 'BSS color technique' since the sensing duration (for the sliding correlator) $\in [71, 142]$ μs. Finally, if the detected signal belongs to a Wi-Fi system, we have to resort to decoding the packet header (BSS color bits) to decide whether the detected signal belongs to a BSS or an OBSS Wi-Fi system and act accordingly as described in Algorithm 1. Although we discussed the CCA adaptation scheme for traditional HD sensing, Algorithm 1 can be easily modified for FD sensing. In this case, the Wi-Fi STA decides whether to continue transmission or quit transmission. Hence, 'transmit' in Algorithm 1 is equivalent to 'continue transmission in the TXOP' for the FD sensing case and 'backoff' is equivalent to 'abort communication' for the FD sensing case. In Section V-B, we optimize γ_{LTEU} via simulations.

Algorithm 1 Adaptive CCA algorithm

```
for each Wi-Fi STA that wants to transmit do
    Wi-Fi STA executes CCA (sense for DIFS) using energy detection
    if RSSI ≤ γ_BSS ≈ −82 dBm then
        Transmit
    else
        Wi-Fi STA executes the LTE-U sliding window correlator
        if correlation metric: M > λ_th (i.e., LTE-U exists) then
            if RSSI < γ_LTEU dBm then
                Transmit
            else
                Backoff (or switch to a new channel)
            end if
        else (correlation metric: M ≤ λ_th)
            Check the BSS color bits
            if BSS color bits indicates OBSS signal then
                if RSSI < γ_OBSS dBm then
                    Transmit
                else
                    Backoff (or switch to a new channel)
                end if
            else (e.g., BSS color bits indicates BSS signal)
                Backoff (or switch to a new channel)
            end if
        end if
    end if
end for
```

V. Performance Evaluation

A. Sliding Window Correlator

We consider a full-duplex enabled Wi-Fi STA with noise floor $\sigma_w^2 = -90$ dBm, and transmitted power $\sigma_s^2 = 20$ dBm. We set $\sigma_{\tilde{I}}^2 = \sigma_w^2$ and vary $\sigma_{\tilde{I}}^2$, β, and χ_w. We analyze how different SIS capabilities, and ISI contamination in the CP affect detector's performance for various setups using numerical and simulation results. We set $L = 500$ and $N = 6400$ taking into account the sampling frequency used in typical Wi-Fi receivers $f_s \geq 20$ MHz and the time length of an LTE-U OFDM symbol (e.g., 72μsec). Unless otherwise stated, all simulation results were generated with 3000 realizations.

In Figures 6 and 7, we set the false alarm detection probability to 0.01 and compute the NP detection threshold as in (14). Next, we evaluate the mis-detection probability through simulation and numerical computations as derived in (8). With zero ISI and RSI, the detection scheme could attain the 10^{-3} mis-detection probability at even low LTE-U signal level such as INR $= -5$ dB (see the No ISI lines in Figure 6). Detector performance degrades as more ISI and RSI are generated.

We analyze the receiver operating characteristic (ROC) performance of the developed detector under different INR conditions (see Figure 8). We evaluate the ROC performance with fixed ISI and RSI values, and we notice a degradation in the false alarm probability as LTE-U signal level decreases below a certain limit (see the INR $= -1$ dB curve in Figure 8).

B. CCA Adaptation Simulation Study

Our objective is to evaluate the trade off between spatial reuse and Wi-Fi/LTE-U fairness by optimizing Wi-Fi CCA threshold. The simulation setup is as follows. We consider a square area of 200×200 square meters, with multiple Wi-Fi and LTE-U devices distributed according to a Poisson point process (PPP). Specifically, we randomly distribute the receivers (e.g., Wi-Fi STAs and UEs) in the specified area according to the PPP with parameter λ_{PPP} ($\lambda_{\text{PPP}} \in [4, 80]$ is a simulation parameter). For a network with N receivers, the number of Wi-Fi STAs equals to the number of UEs. For each receiver, we assign a single transmitter (AP in case of Wi-Fi and HeNB in case of LTE-U) that is uniformly distributed in a square, of length 20 meters, around its corresponding receiver. All HeNBs have a duty cycle (DC), which we vary as a simulation parameter $\in [0.1, 0.9]$.

We model the wireless channels using the path-loss model. The transmission power is 20 dBm, receiver noise power is -90 dBm, carrier frequency is 5 GHz, path-loss exponent is 3.5. Since we are not interested in optimizing γ_{OBSS}, we set $\gamma_{\text{OBSS}} = \gamma_{\text{LTEU}}$ and optimize over γ_{LTEU}. Figure 9 shows the sum throughput of Wi-Fi STAs (R_{WiFi}) and LTE-U UEs (R_{LTEU}) versus λ_{PPP} for different values of γ_{LTEU} at DC$= 0.5$ and DC$= 0.9$, respectively. At DC$= 0.5$, LTE-U achieves much higher throughput than Wi-Fi when $\gamma_{\text{LTEU}} = -82$ dBm, as shown in Figure 9. The reason for this unfair situation for Wi-Fi systems is that Wi-Fi STAs use a very low CCA threshold. Increasing the Wi-Fi CCA threshold to $\gamma_{\text{LTEU}} = -62$ dBm, leans the network throughput towards Wi-Fi because of their

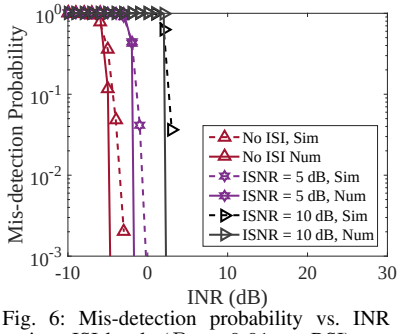

Fig. 6: Mis-detection probability vs. INR for various ISI levels ($P_F = 0.01$, no RSI).

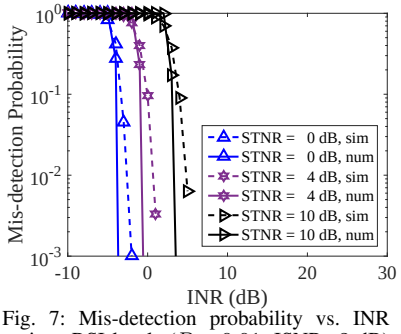

Fig. 7: Mis-detection probability vs. INR for various RSI levels (P_F=0.01, ISNR=2 dB).

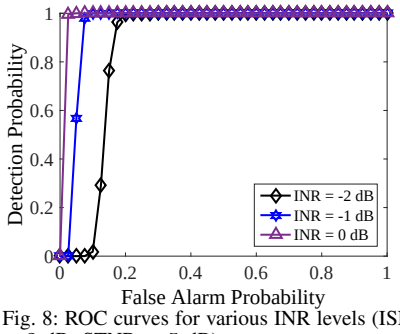

Fig. 8: ROC curves for various INR levels (ISNR = 2 dB, STNR = 5 dB).

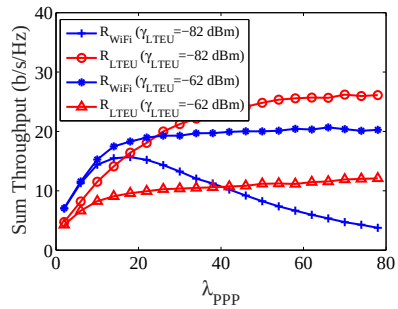

Fig. 9: Throughput vs. λ_{PPP} (DC= 0.5).

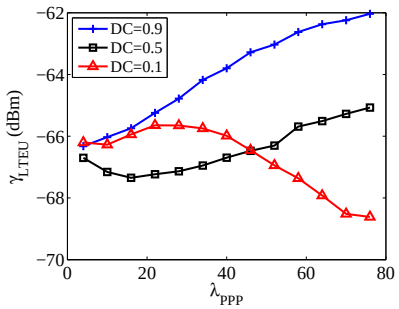

Fig. 10: Optimal CCA threshold vs. λ_{PPP}.

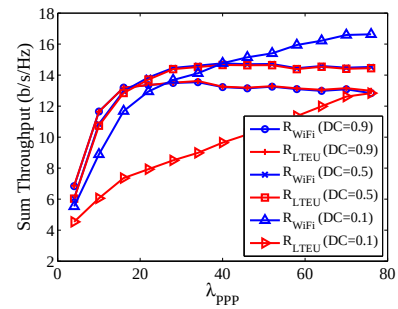

Fig. 11: Fair sum throughput vs. λ_{PPP}.

greediness in using the spectrum. Both CCA threshold values result in unfairness between the two technologies.

Figure 10 shows the optimal values for γ_{LTEU} at different (λ_{PPP}) and at different DC values for the LTE-U systems. For each λ_{PPP} and DC values, our objective is to optimize γ_{LTEU} that minimizes the difference between the sum throughput of Wi-Fi and LTE-U systems (i.e., ensure fairness). Figure 11 shows the optimal sum throughput for both systems. We notice that as the LTE-U DC decreases, γ_{LTEU} decreases since Wi-Fi system is trying to ensure fairness with LTE-U systems. This behavior continues until a certain threshold for the DC of LTE-U systems, where the Wi-Fi systems cannot achieve fairness since the ON period of LTE-U small cells is very small. As shown in Figure 11, Wi-Fi and LTE-U systems achieve almost the same throughput $\forall\gamma_{\text{LTEU}}$ and DC except for very low DC values since the ON period for LTE-U systems is very short.

VI. Conclusions

Traditional TXOP mode in Wi-Fi systems may introduce latency and reduced throughput in case of Wi-Fi/LTE-U coexistence. In this paper, we proposed a modified TXOP mode, in which Wi-Fi STAs carry out simultaneous transmission and sensing by exploiting SIS techniques. We proposed and analyzed a sliding-window correlator detection framework under imperfect SIS and ISI that enables Wi-Fi to distinguish LTE-U signals. We proposed an adaptive CCA threshold scheme that is based on the detected signal type. We optimized, via simulations, the CCA threshold value that maximizes the spatial reuse while maintaining a certain fairness degree between Wi-Fi and LTE-U.

References

[1] "LTE-U technical report: Coexistence study for LTE-U SDL v1.0," https://lteuforum.org, Feb. 2015.

[2] 3GPP, "Study on licensed-assisted access to unlicensed spectrum," 3GPP TR. 36.889 v13.0.0., Jun. 2015.

[3] IEEE, "IEEE–part 11: Wireless LAN medium access control (MAC) and physical layer (PHY) specifications–amendment 4," http://ieeexplore.ieee.org/servlet/opac?punumber=6687185, 2013.

[4] W. Afifi and M. Krunz, "Exploiting self-interference suppression for improved spectrum awareness/efficiency in cognitive radio systems," in *Proc. of the IEEE INFOCOM'13 Conf.*, Apr. 2013, pp. 1258–1266.

[5] T. Riihonen and R. Wichman, "Energy detection in full-duplex cognitive radios under residual self-interference," in *Proc. of the IEEE CROWNCOM'14 Conf.*, June. 2014, pp. 57–60.

[6] W. Afifi and M. Krunz, "Adaptive transmission-reception-sensing strategy for cognitive radios with full-duplex capabilities," in *Proc. of the IEEE DySPAN'14 Conf.*, McLean, VA, Apr. 2014, pp. 149–160.

[7] Huawei and U. of Electronic Science & Technology of China, "Sensing scheme for DVB-T," IEEE Std.802.22-06/0127r1, July. 2006.

[8] S. Chaudhari, V. Koivunen, and H. V. Poor, "Autocorrelation-based decentralized sequential detection of OFDM signals in cognitive radios," *IEEE Trans. Signal Process.*, vol. 57, no. 7, pp. 2690–2700, 2009.

[9] E. Axell and E. G. Larsson, "Optimal and sub-optimal spectrum sensing of OFDM signals in known and unknown noise variance," *IEEE J. Select Areas in Commun.*, vol. 29, no. 2, pp. 290–304, 2011.

[10] V. Syrjälä and M. Valkama, *Coexistence of LTE and WLAN in Unlicensed Bands: Full-Duplex Spectrum Sensing*. Springer International Publishing, 2015, pp. 725–734.

[11] IEEE, "Specification framework for TGax," https://goo.gl/TquK6D, Nov. 2015.

[12] S. Sagari, S. Baysting, D. Saha, I. Seskar, W. Trappe, and D. Raychaudhuri, "Coordinated dynamic spectrum management of LTE-U and Wi-Fi networks," in *Proc. of IEEE DySPAN'2015 Conf.*, Sept. 2015, pp. 209–220.

[13] Y. Li, F. Baccelli, J. G. Andrews, T. D. Novlan, and J. Zhang, "Modeling and analyzing the coexistence of licensed-assisted access LTE and Wi-Fi," in *Proc. of IEEE GC Wkshps'2015 Conf.*, Dec. 2015, pp. 1–6.

[14] S. Nadarajah and S. Kotz, "Exact distribution of the max/min of two gaussian random variables," *IEEE Trans. Very Large Scale Integr. (VLSI) Syst.*, vol. 16, no. 2, pp. 210–212, 2008.

[15] D. V. Hinkley, "On the ratio of two correlated normal random variables," *Biometrika*, vol. 56, no. 3, pp. 635–639, 1969.

[16] G. M. van Kempen and L. J. van Vliet, "Mean and variance of ratio estimators used in fluorescence ratio imaging," *Cytometry*, vol. 39, no. 4, pp. 300–305, 2000.

[17] T. Schmidl and D. Cox, "Robust frequency and timing synchronization for OFDM," *IEEE Trans. Commun*, vol. 45, no. 12, pp. 1613–1621, 1997.